

Received August 13, 2019, accepted August 28, 2019, date of publication September 3, 2019, date of current version September 17, 2019.

Digital Object Identifier 10.1109/ACCESS.2019.2939165

Effect of Imperfect Channel Estimation on the Performance of Cognitive Satellite Terrestrial Networks

XIAOJUAN YAN¹, KANG AN², (Member, IEEE), TAO LIANG², (Member, IEEE),
GAN ZHENG³, (Senior Member, IEEE), AND ZHIQIANG FENG¹

¹Guangxi Ship Digital Design and Advanced Manufacturing Research Center of Engineering Technology, Beibu Gulf University, Qinzhou 535011, China

²Sixty-third Research Institute, National University of Defense Technology, Changsha 410073, China

³Wolfson School of Mechanical, Electrical and Manufacturing Engineering, Loughborough University, Loughborough LE11 3TU, U.K.

Corresponding author: Zhiqiang Feng (fzqsjtu@163.com)

This work was supported in part by the National Natural Science Foundation of China under Grant 61901502 and Grant 51969001, in part by the Research Project of NUDT under Grant ZK18-02-11, and in part by the Guangxi Natural Science Foundation of China under Grant 2016GXNSFAA380188.

ABSTRACT The incorporation of cognitive radio (CR) techniques into satellite communication systems, has been considered as one of the most promising approaches to address the spectrum scarcity, which constitutes an advanced infrastructure known as cognitive satellite terrestrial network (CSTN). Due to the estimation error or feedback delay, perfect channel state information (CSI) of satellite and/or terrestrial links in CSTNs are normally unavailable. This paper investigates the effect of imperfect CSI on the performance of CSTN, where a secondary satellite network coexists with a primary terrestrial network by employing the underlay cognitive mechanism according to which the satellite user is allowed to access the licensed spectrum without deteriorating the operation of terrestrial user. Specifically, we derive the analytical expressions for the outage probability and ergodic capacity of the cognitive network, which provides an efficient approach to jointly evaluate the impacts of imperfect channel estimations for different links on the performance of considered network. Moreover, simple asymptotic outage probability formula in the high signal-to-noise ratio regime is presented to reveal the diversity order and coding gain of the CSTNs. Finally, numerical results are provided to confirm the validity of the theoretical analysis, as well as quantitatively analyze the effects of various system parameters on the performance of the CSTNs with CSI imperfection.

INDEX TERMS Cognitive satellite terrestrial networks, imperfect channel state information, outage probability, ergodic capacity.

I. INTRODUCTION

Satellite communication is capable of providing seamless connectivity and high speed broadband access for worldwide users based on an anywhere-anytime paradigm, especially for users who allocate in the disaster, desert, and/or suburb areas [1]–[3]. However, due to the explosive growing demand for broadband satellite services in recent years, the licensed spectrum of satellite networks seems to be insufficient to meet the forthcoming requirement. Given this fact, exploring new insights and architectures into the utilization of spectrum in satellite communications have challenged the traditional spectrum management approaches [4].

The associate editor coordinating the review of this article and approving it for publication was Francesco Benedetto.

A. BACKGROUND AND MOTIVATION

To alleviate the problem of spectrum scarcity, a cognitive radio (CR) technique, which can increase the spectrum utilization efficiency by adapting its transmission parameters according to the state of the environment [5], has been introduced in the satellite networks to form a new architecture networks, namely as cognitive satellite terrestrial network (CSTN) [6], [7]. In this network, satellite networks can perform as the primary/cognitive networks and share spectrum with terrestrial networks, which act as cognitive/primary networks, on the premise that the QoS of primary networks is ensured [8]. Thus, the spectrum utilization efficiency of primary networks can be enhanced as well as the problem of spectrum scarcity of cognitive networks can be alleviated.

Until now, several ways have been proposed to apply the CR in the CSTN, such as interweave or spectrum sensing [9],

underlay [10], overlay [11], and database approaches [12]. Among those ways, the underlay strategy, with which cognitive user can utilize the licensed terrestrial spectrum resources as long as the harmful mutual interference is properly regulated below a predefined threshold, is the simplest and has been introduced in various networks, such as terrestrial networks [13] and CSTN [10]. On the subject of the underlay based CSTN, many works have been done from various performance metrics, such as outage probability [10], ergodic capacity [14], secure transmission rate [15] with a single antenna eavesdropper, and maximization transmission rate under the constraint of limited transmission power [16] and QoS of cognitive user [17]. Extension work of [15] to a multi-antennas eavesdropper was conducted in [18]. Moreover, some studies have explored the benefit of the underlay based CSTN in various scenarios. The authors in [19] studied the effects of practical hardware impairments on the outage probability of underlay based CSTN. The authors in [20] investigated the specific primary exclusion zone by employing the statistical modeling.

Although those aforementioned works have significantly improved our understanding on the performance of the underlay based CSTNs, they were restricted to the scenarios with perfect channel state information (CSI). In practical scenarios, however, the exact perfect CSI is normally unavailable for satellite communications due to large latency [21], [22]. Moreover, when the CSI of interfering link between the cognitive transmitter and primary receiver is not perfect, the traditional interference power constraint can no longer guarantee the QoS of the primary user [23]. In this regard, channel estimation is a crucial issue for practical implementation of CR approach in the CSTNs, which needs further investigation to deal with the uncertainty of imperfect channel estimations, and thus guarantee the communication quality of the integrated networks.

B. CONTRIBUTION AND NOVELTY

This paper focuses on the uplink CSTN, where the satellite system acts as the cognitive network while the terrestrial system has the role of the primary one. In this work, perfect CSIs of both the cognitive satellite link and terrestrial interference link are considered unavailable due the following facts¹:

- For the cognitive satellite link, perfect CSI estimation is unavailable because of the high latency affected by the round trip propagation delay [21]. For a geostationary satellite, exact CSI experiences a quite delay, while for non-geostationary satellites, the high Doppler shifts may impair the availability of the CSI [22].
- For the terrestrial interference link, the acquisition of instantaneous CSI at the cognitive satellite user may be difficult due to the effect of delay and time-varying nature of the transmitter-receiver pair in different networks, which implies that the feedback overhead should be taken into account [24].

¹The interference from terrestrial terminal to the satellite can be considered to be negligible due to large distance [10],[14]–[17].

- Moreover, channel estimation is not simple and straightforward in CSTNs because of the inherent nature that the cognitive satellite link and terrestrial interference link may experience different signal latency. Hence, separate estimations are required at the satellite user for different links.

Different from the previous works, we focus on the overall effects of imperfect channel estimations on the performance of uplink CSTNs, where the cognitive satellite system is allowed to access the spectral resources of the primary terrestrial system without deteriorating its communication quality. Specifically, our contributions are outlined as follows:

- By considering the inherent nature of both satellite and terrestrial links, an efficient method that separately estimates the cognitive satellite link and terrestrial interference link is employed at the satellite user, where the actual channel gain of the satellite link is estimated by using the training data, while the terrestrial interference channel is obtained by using a feedback link.
- We then derive the novel analytical expressions for the outage probability and ergodic capacity of the cognitive satellite system, which provide efficient means to evaluate the effects of key system parameters, such as number of training symbols and shadowing severities of satellite link, and feedback delay coefficient and interference constraints of terrestrial interference link.
- To gain further insights, the simple asymptotic expressions of outage probability at high SNR are developed to examine the asymptotic behavior of the considered system, which characterize the impact of key system parameters on two important performance metrics, namely the achievable diversity order and coding gain.

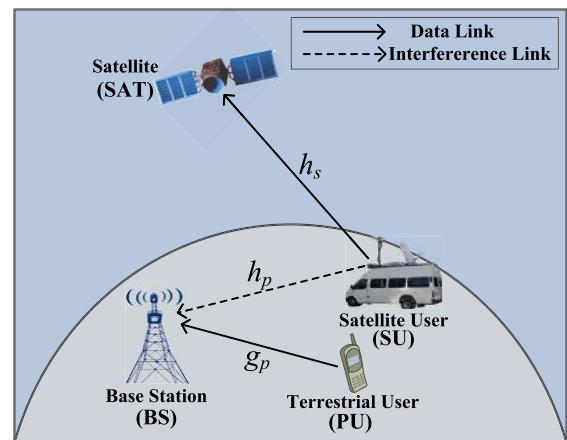


FIGURE 1. System model.

II. SYSTEM MODEL

As shown in Fig. 1, we consider an uplink cognitive satellite terrestrial network, where the terrestrial network acts as the primary system and shares the spectrum resource with the satellite network, which is the secondary system. To improve the overall spectrum efficiency, we assume that the underlay

technique is employed, thus the satellite user utilizes the same spectrum as the terrestrial user simultaneously without deteriorating the communication quality of the latter. From a practical aspect of possible application, the terrestrial system can be a Long-Term Evolution (LTE) system while the satellite system may be a Digital Video Broadcasting-Return channel by Satellite (DVB-RCS) system [16], [17].

Let h_s denote the channel coefficient between satellite and secondary user, and the received signal at the satellite is given by

$$y_s = h_s x + n_s, \quad (1)$$

where x denotes the transmitted signal with average power P_s , and $n_s \sim \mathcal{N}_C(0, \sigma_B^2)$ represents the zero mean additive white Gaussian noise (AWGN). Recall that in an underlay scheme, the interference at the BS caused by the cognitive user must not exceed a predefined interference power constraint Q . To achieve this, satellite user must adapt its transmit power based on the instantaneous CSI of the mutual interference link, namely, [10], [14]

$$P_s = \min \left(\frac{Q}{|h_p|^2}, P_t \right) \quad (2)$$

where P_t is the maximum allowable transmit power by the power amplifier, h_p the terrestrial interference link from the satellite user to BS. In the specific scenario, we consider that the satellite terminal is a mobile/portable terminal and therefore employ a widely-employed Shadowed-Rician (SR) fading model for the cognitive satellite network with closed form, which can be used either for mobile/portable terminals or for fixed terminals operating in various propagation environments [10], [14]–[17]. Moreover, without loss of generality, the Rayleigh fading channel is considered for the terrestrial interference link [10].

As discussed before, the perfect CSIs of both h_s and h_p are normally impossible to obtain at the cognitive satellite user. For the considered cognitive architecture, due to the inherent different nature of both links, the overall communication for channel estimation and data transmission can be summarized in the following protocols:

- **Channel Estimation of Satellite Uplink:** In this phase, the channel estimation is performed by using forward training, through which satellite user transmits pilots to the satellite, and then the satellite estimates the uplink channel and sends the estimated value over the downlink [21], [22]. However, due to the large propagation delay, the estimation of the uplink channel would become outdated.
- **Channel Estimation of Interference Link:** Due to the mobility of the nodes among different networks, the CSI of mutual interference link between the satellite user and BS would be outdated. Generally, it is considered that the channel knowledge of the interference link at the secondary transmitter is provided by using an existing feedback link [16], [17].

- **Data Transmission:** Finally, the secondary user transmits the desired signal to the satellite by employing a power control scheme without affecting the operation of the primary network. An underlay spectrum sharing approach is adopted, where the satellite user is allowed to access the licensed spectrum, simultaneously with the primary user, as long as it does not impose a harmful interference beyond a predefined threshold at the BS.

In what follows, these three phases will be described in detail.

A. CHANNEL ESTIMATION OF SATELLITE UPLINK

Let the satellite user transmit $L \in \mathbb{Z}^+$ training symbols to the satellite in L time slots, therefore the receiver signal at the satellite can be expressed as [21]

$$r_i = h_s s_i + n_{s,i}, \quad i = 1, 2, \dots, L \quad (3)$$

By employing an efficient joint detection processing along with (1) and (3) [22], the expression of the conditional probability density function (PDF) for the maximum likelihood (ML) detector is derived as

$$\ln f_{(y_s, r_1, r_2, \dots, r_L)}(y_s, r_1, r_2, \dots, r_L) = X - |y_s - h_s x|^2 - \sum_{i=1}^L |r_i - h_s s_i|^2, \quad (4)$$

where $X = \ln \left(\frac{1}{\sqrt{\pi} \sigma^2} \right)$. By taking the derivative of (4) with respect to h_s and equating it to zero, it can further rewritten as

$$\tilde{h}_s = \frac{x^* y_s + \sum_{i=1}^L s_i^* r_i}{L + 1}. \quad (5)$$

Combining (1) and (5), we further get

$$\tilde{h}_s = h_s + \tilde{n}_s, \quad (6)$$

where $\tilde{n}_s = \left(x^* n_s + \sum_{i=1}^L s_i^* n_{s,i} \right) / (L + 1)$ is the estimation error component of exact channel h_s satisfying $E[|\tilde{n}_s|^2] = \sigma^2 / (L + 1)$. From (4), we can get that in case of perfect CSI estimation, the decision variable for symbol x is

$$\Lambda = \arg \min_{\tilde{x}} \left\{ |y_s - h_s \tilde{x}|^2 + \sum_{i=1}^L |r_i - h_s s_i|^2 \right\}. \quad (7)$$

Since perfect CSI is not available at the satellite, we replace h_s with \tilde{h}_s in (7). Thus, the data decision variable with estimated CSI can be written as

$$\Lambda = \arg \min_{\tilde{x}} \left\{ |h_s (x - \tilde{x}) - \tilde{n}_s \tilde{x} + n_s|^2 + \sum_{i=1}^L |n_{s,i} - \tilde{n}_s s_i|^2 \right\}. \quad (8)$$

Note that $\sum_{i=1}^L |n_{s,i} - \tilde{n}_s s_i|^2$ is independent of the x , so it does not contribute to the effective decision metric. Thus, the estimated SNR can be written as $\tilde{\gamma}_s = \frac{|h_s|^2}{\sigma^2(1 + \frac{1}{L+1})}$ [21]. After estimating the uplink channel, the estimated value will be sent

over the downlink [21], [22]. To this end, the instantaneous received SNR at the satellite can be written as

$$\gamma_s = \frac{P_s}{\sigma^2} |\tilde{h}_s|^2, \quad (9)$$

where $|\tilde{h}_s|^2 = \frac{|h_s|^2}{(1+\frac{1}{L+1})}$ and P_s is the transmit power at the satellite user.

B. CHANNEL ESTIMATION OF TERRESTRIAL INTERFERENCE LINK

The channel gain of the terrestrial interference link may not be available to the satellite user. The outdated channel gains would lead to an overestimation or underestimation of the induced interference at the BS, which leads to the degradation either of the satellite's ergodic capacity, or the terrestrial system's communication quality [16]. For the scenario with overestimation, the available power resource at satellite user cannot be fully utilized. On the other hand, when the mutual interference is underestimated, the interference power constraint with perfect CSI assumption will cause an increase of outage probability of the terrestrial BS due to the higher transmit power adopted at the satellite user. Please note that this model can be used to access the impact of several factors on the CSI, including channel estimation error, mobility and feedback delay ([23] and the references therein). Due to the imperfect feedback channel, the satellite user can only access the outdated CSI, which can be described using the correlation model as follows [23]²

$$\tilde{h}_p = \rho h_p + \sqrt{1 - \rho^2} n_p, \quad (10)$$

where \tilde{h}_p denotes the delayed version of h_p , n_p is the complex Gaussian variable having the same variance as h_p . According to Jakes' autocorrelation model [24], the feedback delay coefficients between \tilde{h}_p and h_p is expressed as $\rho = J_0(2\pi f\tau)$, and f is the maximum Doppler frequency, τ is the delay coefficient between the actual instant and the transmission instant, $J_0(\cdot)$ is the zeroth-order Bessel function of the first kind [28, eq. (8.411)].

With outdated CSI, it is not possible to meet the instantaneous interference power constraint. To eliminate the negative effects, we take a probabilistic approach as in [23], where the satellite user adapts its power with a protection mechanism based on a modified estimation of the terrestrial link's CSI as

$$P_s = \min \left(\kappa \frac{Q}{|\tilde{h}_p|^2}, P_t \right), \quad (11)$$

²The effect of imperfect CSI on system performance were investigated in [25]–[27] by defining a confined region for the channel variations, which refers to the bounded CSI error model, and/or by assuming that the channel estimation error obeys the Gaussian distribution, namely gaussian CSI error model. These models are suitable for the robust system design within a certain ranges of uncertainty, which can be a potential research area in our future work.

with κ being the power margin factor due to imperfect channel estimation. According to [23], the power margin factor can be numerically derived by solving the following equation as

$$\begin{aligned} \varepsilon = & 1 - \exp\left(-\frac{Q}{\lambda P_t}\right) + \exp\left(-\frac{Q}{\lambda P_t}\right) \\ & \times Q\left(\sqrt{\frac{2\rho^2 Q}{\lambda P_t(1-\rho^2)}}, \sqrt{\frac{2\kappa Q}{\lambda P_t(1-\rho^2)}}\right) \\ & + \frac{t}{r} Q\left(\sqrt{\frac{(u-r)Q}{2P_t}}, \sqrt{\frac{(u+r)Q}{2P_t}}\right) \\ & - \frac{1}{2}\left(1 + \frac{t}{r}\right) \exp\left(-\frac{uQ}{2P_t}\right) I_0\left(\frac{2\rho Q\sqrt{\kappa}}{(1-\rho^2)\lambda P_t}\right), \quad (12) \end{aligned}$$

where ε is the pre-selected outage probability required at the primary BS with

$$u = \frac{2}{\lambda} \left(1 + \frac{\rho^2}{1-\rho^2} + \frac{\kappa}{(1-\rho^2)} \right), \quad (13a)$$

$$t = \frac{2}{\lambda} \left(1 + \frac{\rho^2}{1-\rho^2} - \frac{\kappa}{(1-\rho^2)} \right), \quad (13b)$$

$$r = \sqrt{s^2 - \frac{16\rho^2\kappa}{\lambda^2(1-\rho^2)^2}}, \quad (13c)$$

and

$$Q(a, b) = \int_0^\infty x \exp\left(-\frac{a^2 + x^2}{2}\right) I_0(ax) dx, \quad (14)$$

is the Marcum Q -function of first-order, and $I_0(\cdot)$ is the zeroth-order modified Bessel function of the first kind [28, eq. (8.431.1)].

C. DATA TRANSMISSION

In the data transmission phase, by combining (9) and (11), the received end-to-end SNR at the satellite can be expressed as

$$\gamma_s = \min \left(\kappa \frac{Q}{|\tilde{h}_p|^2}, P_t \right) \frac{|\tilde{h}_s|^2}{\sigma^2} = \min \left(\frac{\bar{\gamma}_Q}{|\tilde{h}_p|^2}, \bar{\gamma}_t \right) |\tilde{h}_s|^2, \quad (15)$$

where $\bar{\gamma}_Q = \frac{\kappa Q}{\sigma^2}$ and $\bar{\gamma}_t = \frac{P_t}{\sigma^2}$.

III. PERFORMANCE EVALUATION

In this section, we present a comprehensive investigation on the effect of imperfect CSI on the performance of CSTNs in terms of key performance metrics, including outage probability, ergodic capacity as well as asymptotic outage probability in the high SNR regime. Before delving into the details, we first present the statistical properties of satellite and terrestrial links, which will be frequently used in the subsequent derivations.

A. PRELIMINARY RESULTS

In the Shadowed-Rician model, the amplitude of the shadowed line-of-sight (LoS) signal follows the Nakagami distribution, and the multi-path component of the signal envelope, that may occur because of the scatterers near the transmitter (e.g. trees, buildings), is characterised by Rayleigh distribution. This fading model can accurately describe the land mobile satellite (LMS) channel with significantly less computational burden [29], which is expected to play a prominent role in future satellite communication systems [10], [14]–[17].

Lemma 1: For scenarios with imperfect CSI estimation, the PDF of channel power gain \tilde{h}_s in (15) is given by

$$f_{|\tilde{h}_s|^2}(x) = \alpha \exp\left(-\left(1 + \frac{1}{L+1}\right)\beta x\right) \times {}_1F_1\left(m_1; 1; \left(1 + \frac{1}{L+1}\right)\delta x\right), \quad (16)$$

where ${}_1F_1(a; b; c)$ represents the confluent hypergeometric function [28, eq. (9.210.1)], and α , β and δ are, respectively, given by

$$\alpha = 2bm / (2bm(2bm + \Omega)), \quad (17a)$$

$$\beta = 1/2b, \quad (17b)$$

$$\delta = \Omega/2b(2bm + \Omega), \quad (17c)$$

with Ω being the average power of the LoS component, $2b$ the average power of the multipath component, and m the Nakagami parameter corresponding to the fading severity. According to [17], [29], the channel parameters of the satellite links closely depend on the elevation angle θ , which can be calculated over the range $20^\circ \leq \theta \leq 80^\circ$ by the following expressions

$$\begin{aligned} b(\theta) &= -4.7943 \times 10^{-8}\theta^3 + 5.5784 \times 10^{-6}\theta^2 \\ &\quad - 2.1344 \times 10^{-4}\theta + 3.2710 \times 10^{-2}, \\ m(\theta) &= 6.3739 \times 10^{-5}\theta^3 + 5.8533 \times 10^{-4}\theta^2 \\ &\quad - 1.5973 \times 10^{-1}\theta + 3.5156, \\ \Omega(\theta) &= 1.4428 \times 10^{-5}\theta^3 - 2.3798 \times 10^{-3}\theta^2 \\ &\quad + 1.2702 \times 10^{-1}\theta - 1.4864 \end{aligned} \quad (18)$$

Proof: The desired result can be obtained by using (15) and [28, eq. (3.351.2)] along with algebraic manipulations.

Lemma 2: For scenarios with imperfect CSI estimation, the cumulative distribution function (CDF) of channel power gain \tilde{h}_s in (15) can be derived as

$$F_{|\tilde{h}_s|^2}(x) = 1 - \alpha \exp\left(-\left(1 + \frac{1}{L+1}\right)(\beta - \delta)x\right) \times \sum_{k=0}^{m-1} \sum_{l=0}^k \Xi(k, l)x^l, \quad (19)$$

where α , β and δ are defined in lemma 1 and

$$\begin{aligned} \Xi(k, l) &= \sum_{k=0}^{m-1} \frac{(-1)^k (1-m)_k \delta^k}{k!} \sum_{l=0}^k \frac{1}{l!} \\ &\quad \times \left(1 + \frac{1}{L+1}\right)^l (\beta - \delta)^{-k+l-1}. \end{aligned} \quad (20)$$

Proof: The proof can be found in [1].

Moreover, since the terrestrial interference link \tilde{h}_p follows the Rayleigh fading with exponential distribution, the PDF and CDF of the channel power gain $|\tilde{h}_p|^2$ in (15) is defined as

$$f_{|\tilde{h}_p|^2}(x) = \frac{1}{\lambda} \exp\left(-\frac{x}{\lambda}\right), \quad (21)$$

$$F_{|\tilde{h}_p|^2}(x) = 1 - \exp\left(-\frac{x}{\lambda}\right), \quad (22)$$

where λ denotes the average power of terrestrial interference link.

In the following sections, based on these statistical properties of the fading channels, we will provide a comprehensive performance evaluation of the considered CSTNs with imperfect CSI.

B. OUTAGE PROBABILITY

In wireless communications, the outage probability is an important QoS performance measure, which is defined as the probability that the instantaneous SNR γ_s falls below an acceptable threshold γ_{th} , namely,

$$P_{out} = \Pr(\gamma_s \leq \gamma_{th}) = F_{\gamma_s}(\gamma_{th}), \quad (23)$$

where $F_{\gamma_s}(x)$ denotes the CDF of γ_s . In what follows, we will derive the exact CDF of γ_s in the following theorem.

Theorem 1: The analytical expression of $F_{\gamma_s}(x)$ for considered CSTNs with imperfect CSI can be expressed as

$$\begin{aligned} F_{\gamma_s}(x) &= 1 - \alpha \sum_{k=0}^{m-1} \sum_{l=0}^k \Xi(k, l) \left\{ \left(\frac{x}{\tilde{\gamma}_t}\right)^l \left[1 - \exp\left(-\frac{\tilde{\gamma}_Q}{\lambda \tilde{\gamma}_t}\right)\right] \right. \\ &\quad \times \exp\left(-\left(1 + \frac{1}{L+1}\right)\frac{(\beta - \delta)x}{\tilde{\gamma}_t}\right) \\ &\quad + \frac{1}{\lambda} \left(\frac{x}{\tilde{\gamma}_Q}\right)^l \exp\left(-\frac{\tilde{\gamma}_Q}{\tilde{\gamma}_t} \left(\left(1 + \frac{1}{L+1}\right)\frac{(\beta - \delta)x}{\tilde{\gamma}_Q} + \frac{1}{\lambda}\right)\right) \\ &\quad \left. \times \sum_{i=0}^l \frac{l!}{i!} \left(\frac{\tilde{\gamma}_Q}{\tilde{\gamma}_t}\right)^i \left(\left(1 + \frac{1}{L+1}\right)\frac{(\beta - \delta)x}{\tilde{\gamma}_Q} + \frac{1}{\lambda}\right)^{-l+i-1} \right\}. \end{aligned} \quad (24)$$

Proof: The proof can be found in Appendix A.

C. ERGODIC CAPACITY

The ergodic capacity is defined as the expected value of instantaneous mutual information of the end-to-end SNR γ_s , namely

$$C_s = E [\log_2 (1 + \gamma_s)] = \int_0^\infty \log_2 (1 + x) f_{\gamma_s} (x) dx. \quad (25)$$

By applying the integration by parts approach, (25) can be further rewritten as

$$\begin{aligned} C_s &= \log_2 (1 + x) \left[F_{\gamma_s} (x) - 1 \right]_0^\infty \\ &\quad - \frac{1}{\ln 2} \int_0^\infty \frac{1}{1 + x} \left[F_{\gamma_s} (x) - 1 \right] dx \\ &= \frac{1}{\ln 2} \int_0^\infty \frac{1}{1 + x} \left[1 - F_{\gamma_s} (x) \right] dx. \end{aligned} \quad (26)$$

Theorem 2: The analytical expression of C_s for the considered CSTNs with imperfect CSI can be computed as

$$\begin{aligned} C_s &= \frac{\alpha}{\ln 2} \sum_{k=0}^{m-1} \sum_{l=0}^k \Xi (k, l) \left\{ \frac{\Gamma (l + 1)}{\bar{\gamma}_t^l} \left[1 - \exp \left(-\frac{\bar{\gamma}_Q}{\lambda \bar{\gamma}_t} \right) \right] \right. \\ &\quad \times U \left(l + 1, l + 1, \left(1 + \frac{1}{L + 1} \right) \frac{(\beta - \delta)}{\bar{\gamma}_t} \right) \\ &\quad - \frac{1}{\lambda} \exp \left(-\frac{\bar{\gamma}_Q}{\lambda \bar{\gamma}_t} \right) \sum_{i=0}^k \frac{k! \rho^{k-i+1} \bar{\gamma}_Q^{i-l}}{i! \Gamma (k - i + 1) \bar{\gamma}_t^i} \\ &\quad \times \left(\left(1 + \frac{1}{L + 1} \right) \frac{(\beta - \delta)}{\bar{\gamma}_t} \right)^{-(l+1)} \\ &\quad \left. \times G_{1, [1:1], 0, [1:1]}^{1, 1, 1, 1, 1} \left[\begin{matrix} \frac{\lambda \bar{\gamma}_t}{\bar{\gamma}_Q} \\ 1 \\ \left(1 + \frac{1}{L + 1} \right) \frac{(\beta - \delta)}{\bar{\gamma}_t} \end{matrix} \middle| \begin{matrix} l + 1 \\ -k + i; 0 \\ - \\ 0; 0 \end{matrix} \right] \right\}, \end{aligned} \quad (27)$$

where $U (\cdot, \cdot, \cdot)$ denotes the confluent hypergeometric function, and $G_{1, [1:1], 0, [1:1]}^{1, 1, 1, 1, 1} [\cdot]$ is the Meijer-G function of two variables [32].

Proof: The proof can be found in Appendix B.

D. ASYMPTOTIC OUTAGE PROBABILITY AT HIGH SNR

Here, we study the asymptotic outage probability of the CSTNs with imperfect CSI and thereby reveal two important performance merits: diversity order and coding gain, where the diversity order specifies the slope of the decay, and the coding gain particularizes the relative horizontal shift at asymptotically high values of SNR.

We look into the asymptotic regime by considering two practical scenarios, namely, 1) proportional interference power constraint, where the interference power constraint Q is proportional to the maximum transmit power P_t , i.e., $\bar{\gamma}_Q = \eta \bar{\gamma}_t$ with η being a positive constant, and 2) fixed interference power constraint, where the peak interference power Q is fixed and independent of the maximum transmit power P_t .

1) PROPORTIONAL INTERFERENCE POWER CONSTRAINT

Resorting to the same assumption as in [10], we consider the proportional interference power constraint scenario, which means that the BS is able to tolerate a high amount of interference from the satellite user.

Theorem 3: For the scenario with proportional interference power constraint at the BS, the analytical expression of P_{out}^∞ at high SNR for the considered CSTNs with imperfect CSI can be expressed as

$$P_{out}^\infty \approx \Delta \left(\frac{\gamma_{th}}{\bar{\gamma}_t} \right), \quad (28)$$

where

$$\Delta = \alpha \left(1 + \frac{1}{L + 1} \right) \left\{ \left[1 - \exp \left(-\frac{\eta}{\lambda} \right) \right] + \frac{\lambda + \eta}{\eta} \exp \left(-\frac{\eta}{\lambda} \right) \right\}, \quad (29)$$

Proof: The proof can be found in Appendix C. Based on Theorem 3, we present the following corollary and remark.

Corollary 1: The diversity order G_d and coding gain G_c of the considered CSTNs with ICSI are given by

$$G_d = 1, \text{ and } G_c = \frac{\Delta^{-1}}{\gamma_{th}}, \quad (30)$$

Proof: By representing asymptotic OP in (28) as $P_{out}^\infty (\gamma_{th}) \approx (G_c \bar{\gamma}_t)^{-G_d}$, the diversity order and coding gain of the CSTNs can be easily extracted.

Remark 1: The key insights of Corollary 1 shows that when the interference power constraint Q is proportional to the maximum transmit power P_t , the achievable diversity order G_d remains one, which suggests that the imperfect CSI of both the satellite link and terrestrial interference link does not affect the diversity order. That is to say, the number of training symbols L and feedback delay coefficient ρ , have no impact on the diversity order of the cognitive satellite network. Instead, it degrades the outage performance by degrading the coding gain, which can be quantitatively evaluated through (29).

2) PEAK INTERFERENCE POWER CONSTRAINT

In this subsection, we focus on the peak interference power constraint, where $\bar{\gamma}_Q$ remain fixed while $\bar{\gamma}_t$ grows large in the high SNR regime.

Theorem 4: For the scenario with peak interference power constraint at the BS, the analytical expression of P_{out}^∞ at high SNR for the considered CSTNs with imperfect CSI can be given by

$$P_{out}^\infty \approx \Theta \left(\frac{\gamma_{th}}{\bar{\gamma}_t} \right) + \Xi \left(\frac{\gamma_{th}}{\bar{\gamma}_Q} \right), \quad (31)$$

where

$$\Theta = \alpha \left(1 + \frac{1}{L + 1} \right) \left[1 - \exp \left(-\frac{\bar{\gamma}_Q}{\lambda \bar{\gamma}_t} \right) \right], \quad (32)$$

and

$$\Xi = \alpha \left(1 + \frac{1}{L + 1} \right) \exp \left(-\frac{\bar{\gamma}_Q}{\lambda \bar{\gamma}_t} \right) \left(\lambda + \frac{\bar{\gamma}_Q}{\bar{\gamma}_t} \right). \quad (33)$$

Proof: The result can be obtained by following similar procedures as the proof of Theorem 3. From Theorem 4, we have the following remark.

Corollary 2: When $\bar{\gamma}_t$ approaches infinity, the first term in (31) turns to zero, namely,

$$P_{out}^{\infty} \xrightarrow{\bar{\gamma}_t \rightarrow \infty} \Xi \left(\frac{\gamma_{th}}{\bar{\gamma}_Q} \right). \quad (34)$$

Apparently, the diversity order G_d of the considered CSTNs equals to zero. This means that an outage floor is presented, which is determined by the the second terms in (31).

Remark 2: The observation of Corollary 2 indicates that when the peak interference power constraint Q is employed, the outage performance becomes saturated at high SNR, which demonstrates that only zero diversity order can be achieved by the considered CSTNs regardless of the CSI concerning the satellite link and terrestrial interference link. This is because the interference temperature constraint Q at the BS becomes the dominant factor to determine the maximum allowed transmit power at the satellite user.

IV. SIMULATION RESULTS

In this section, we provide simulation and numerical results to examine the impacts of various parameters on the performance of the considered CSTNs with CSI imperfection. Without loss of generality, we set the predefined threshold $\gamma_{th} = 1$ dB, and $\lambda = 1$. The simulation results are obtained by performing 10^6 channel realizations, and the different values of satellite elevation angle $\theta = 20^\circ, 40^\circ, 60^\circ$ are corresponding to the heavy, average and light shadowing severities of the satellite links [29], [33], [34].

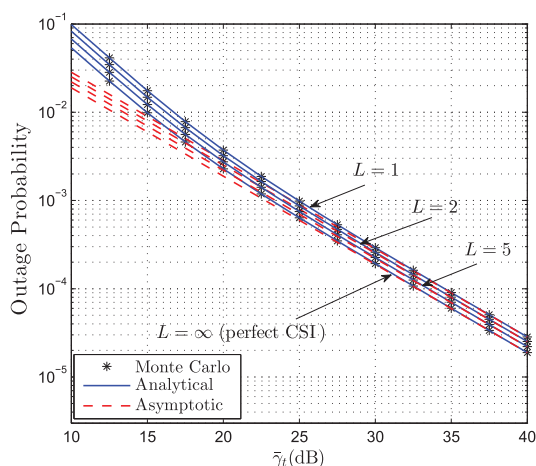


FIGURE 2. Outage probability of cognitive satellite network for different values of Q and L under proportional interference constraint with $\theta = 40^\circ, \eta = 1, \varepsilon = 10\%$ and $\rho = 1$.

To begin with, Fig. 2 plots the exact and asymptotic outage probability of the cognitive satellite network under proportional interference power constraint for different values of Q and L . Here, the cases that satellite uplink has the knowledge of perfect CSI (denoted as $L = \infty$) are also provided

as benchmarks for performance comparison. As shown in this figure, we see an excellent match between the simulation results and the analytical curves, while the asymptotic curves match well with the exact results in the high SNR regime. Besides, the outage performance with imperfect CSI of satellite uplink gradually approaches toward the perfect CSI case with the increase of training symbol L , which can be explained by the fact that more training symbols L means more precise channel estimation at the satellite. In addition, from the asymptotic analysis, we can find that the quality of channel estimation for satellite link does not affect the diversity order of the considered CSTNs.

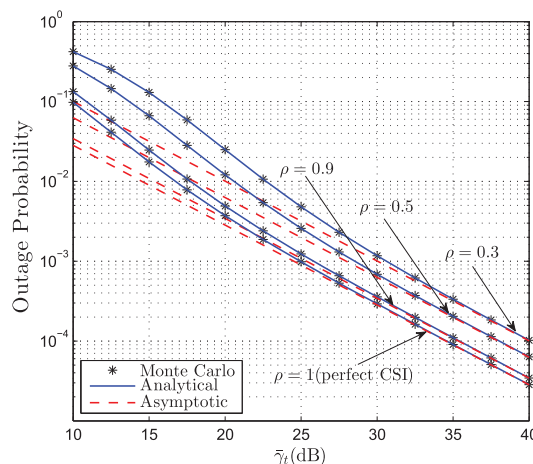


FIGURE 3. Outage probability of cognitive satellite network for different feedback delay coefficient ρ under proportional interference constraint with $\theta = 40^\circ, \eta = 1, \varepsilon = 10\%$ and $L = 2$.

Fig. 3 shows the outage probability of cognitive satellite network for different feedback delay coefficient of terrestrial interference link under proportional interference constraints, where $\rho = 1$ denotes the ideal case without feedback delay. From the figure, we can observe that the outage probability improves when ρ increases, this is quite intuitive since the larger ρ is, the smaller the feedback delay would be presented. Moreover, we see that the curves associated with outdated CSI achieve the same diversity order of one, which confirms the analytical findings of Theorem 3 that the feedback delay leads to the system degradation by reducing the coding gain.

Fig. 4 illustrates the effect of pre-selected interference outage constraint factor ε on the performance of cognitive satellite network under the proportional interference constraint. As we can readily observe, the outage probability associated with the case $\varepsilon = 10\%$ is strictly smaller than that of the case 1% , which indicates that allowing a less stringent interference outage constraint could significantly improve the outage performance of the cognitive satellite user. Moreover, we can also find that, for the small feedback delay coefficient, i.e., $\rho < 0.5$, the improvement of the accuracy of the feedback CSI yields marginal outage

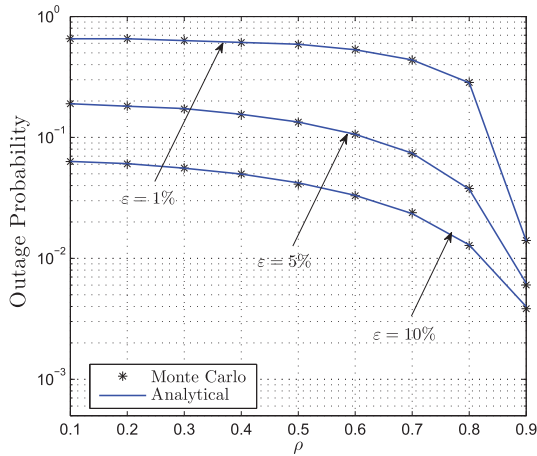


FIGURE 4. Outage probability of cognitive satellite network for different interference outage constraint factor ε under proportional interference constraint with $\theta = 40^\circ$, $\eta = 1$ and $L = 2$.

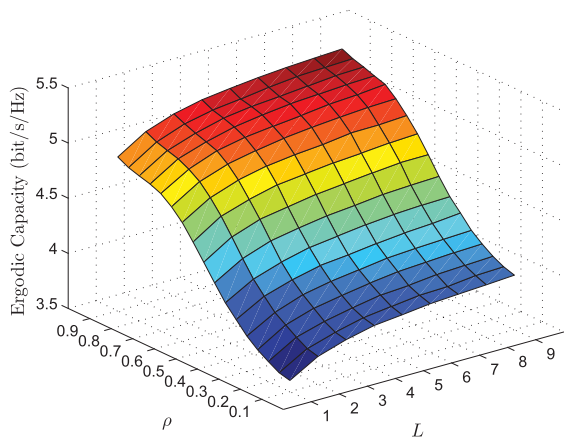


FIGURE 5. Ergodic capacity of cognitive satellite network for different training symbols L and feedback delay coefficient ρ under proportional interference constraint with $\theta = 40^\circ$, $\eta = 1$ and $\gamma_t = \gamma_Q = 20$ dB.

probability enhancement. In contrast, for the large feedback delay coefficient, i.e., $\rho > 0.7$, a relatively small increase of ρ provides a substantial decrease of the outage probability.

Fig. 5 depicts the ergodic capacity (in bit/s/Hz) of cognitive satellite network for different training symbols L and feedback delay coefficient ρ under proportional interference constraint. Apparently, with the secondary satellite user employing partial CSIs of terrestrial interference link, the system capacity of cognitive satellite network degrades with the decrease of ρ . In this case, the actual interference caused to the primary network exceeds the expected level. This is not acceptable from the BS's point of view, and a possible solution is to demand an additional power margin factor κ . Moreover, the CSI imperfection of satellite uplink would be alleviated with more transmitted training symbol at the ES.

Fig. 6 plots the exact and asymptotic outage probability of the cognitive satellite network under the peak interference power constraint, where the cases of no interference temperature constraint and the perfect CSI of satellite normal link (denoted as $L = \infty$) are plotted for comparison.

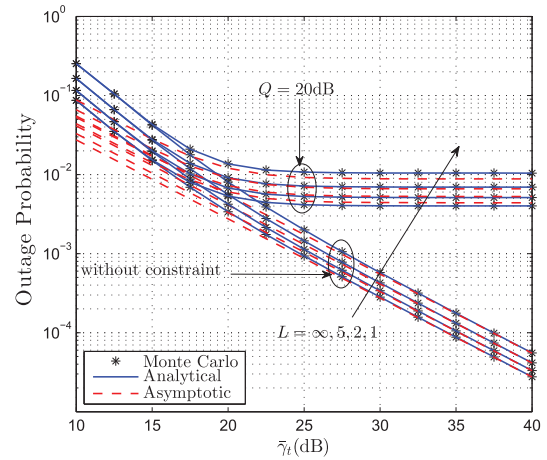


FIGURE 6. Outage probability of cognitive satellite network for different values of L under peak interference constraint with $\theta = 40^\circ$, $\varepsilon = 10\%$ and $\rho = 1$.

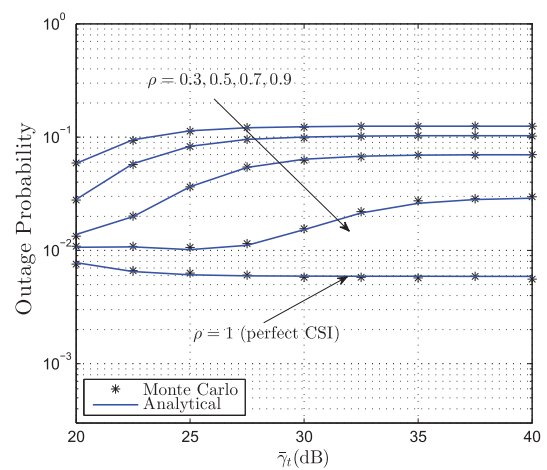


FIGURE 7. Outage probability of cognitive satellite network for different feedback delay coefficient ρ under the peak interference constraint with $\theta = 40^\circ$, $\varepsilon = 10\%$, $Q = 20$ dB and $L = 2$.

As can be clearly seen, the outage probability of the cognitive satellite network under an interference temperature constraint is generally inferior to that of the network without such a constraint. Besides, the outage probability of the CR system becomes saturated due to the interference temperature constraint, which verifies the asymptotic results shown in Theorem 4 and Remark 2. Although our findings indicate that when the interference power constraint is fixed, an outage error floor exists and the diversity gain is lost, the outage performance can be improved by adopting training symbol. Fig. 7 examines the impact of feedback delay coefficient ρ of the terrestrial interference link on the outage probability of the cognitive satellite network under the peak interference constraint. From the figure, we observe that the imperfect CSI of the terrestrial interference link significantly degrades the performance of the cognitive network. Specifically, with the increase of P_t , a small power margin coefficient κ will be required, which subsequently degrades P_s as shown in (15).

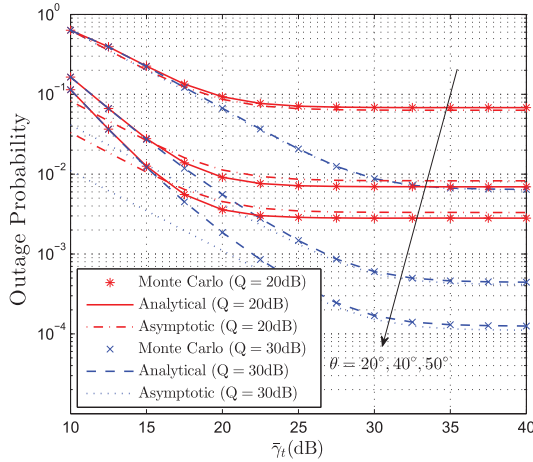


FIGURE 8. Outage probability of cognitive satellite network for different elevation angle θ under peak interference constraint with $\epsilon = 10\%$, $\rho = 1$ and $L = 2$.

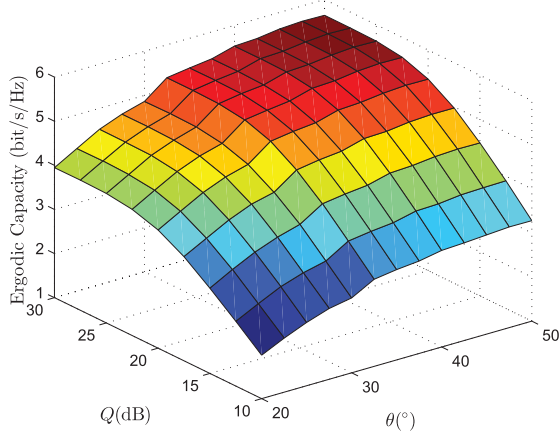


FIGURE 9. Ergodic capacity of cognitive satellite network for different values of Q and elevation angle θ under peak interference constraint with $\epsilon = 10\%$, $\rho = 1$ and $L = 2$.

Fig. 8 describes the outage probability of the cognitive satellite network for different elevation angles of the satellite user. For increasing values of the elevation angle, a reduced outage performance can be achieved. This is an expected result since higher elevation angles correspond to better propagation conditions, thus resulting in an enhanced outage performance. Besides, it can be seen that with the increase of θ , although the diversity order remains one, a noticeable decrease of outage occurs. This is because the primary interfering satellite link degrades the system performance by reducing the code gain. Furthermore, the outage error saturation can be improved by relaxing the interference temperature constraint, i.e., Q gets larger. Finally, Fig. 9 illustrates the ergodic capacity (in bit/s/Hz) of the cognitive satellite network for different values of Q and a wide range of elevation angle θ under the peak interference constraint. Similar to the outage performance, an improved satellite system’s capacity can be obtained for increasing values of Q and θ .

V. CONCLUSION

In this paper, we have investigated the impact of imperfect CSI on the performance of cognitive satellite terrestrial network with respect to both proportional and peak interference constraints. Specifically, exact analytical expressions for the outage probability and ergodic capacity of the cognitive satellite network have been derived, whose validity has been confirmed by Monte Carlo simulations. Furthermore, simple asymptotic expressions for the outage probability at high SNR was also presented, which give useful insights on the achievable diversity order and coding gain. Our findings reveal that under the proportional interference constraint, the achievable diversity order remains one, regardless of imperfect CSI for both the cognitive satellite link and terrestrial interference link. However, under the peak interference power constraint, the outage error floor appears at the high SNR and the achievable diversity order reduces to zero regardless of the CSI imperfections concerning both links.

APPENDIX A PROOF OF THEOREM 2

Based on (15) and the concept of conditional probability, the $F_{\gamma_s}(x)$ can be reexpressed as the sum of the following probabilities,

$$F_{\gamma_s}(x) = \underbrace{\Pr\left(\bar{\gamma}_t |\tilde{h}_s|^2 \leq x, \bar{\gamma}_t \leq \frac{\bar{\gamma}_Q}{|\tilde{h}_p|^2}\right)}_{I_1} + \underbrace{\Pr\left(\frac{\bar{\gamma}_Q}{|\tilde{h}_p|^2} |\tilde{h}_s|^2 \leq x, \bar{\gamma}_t > \frac{\bar{\gamma}_Q}{|\tilde{h}_p|^2}\right)}_{I_2}. \quad (A.1)$$

Then, due to independent nature of \tilde{h}_p and \tilde{h}_s , I_1 and I_2 can be rewritten as

$$I_1 = \int_0^{\bar{\gamma}_Q/\bar{\gamma}_t} F_{|\tilde{h}_s|^2}\left(\frac{x}{\bar{\gamma}_t}\right) f_{|\tilde{h}_p|^2}(y) dy, \quad (A.2)$$

and

$$I_2 = \int_{\bar{\gamma}_Q/\bar{\gamma}_t}^{\infty} F_{|\tilde{h}_s|^2}\left(\frac{xy}{\bar{\gamma}_Q}\right) f_{|\tilde{h}_p|^2}(y) dy. \quad (A.3)$$

By using (19) and (21) along with [28, eqs. (3.351.2), (3.351.3)], I_1 and I_2 can be, respectively, computed as

$$I_1 = F_{|\tilde{h}_p|^2}\left(\frac{\bar{\gamma}_Q}{\bar{\gamma}_t}\right) - \alpha \exp\left(-\left(1 + \frac{1}{L+1}\right) \frac{(\beta - \delta)x}{\bar{\gamma}_t}\right) \times \sum_{k=0}^{m-1} \sum_{l=0}^k \Xi(k, l) \left(\frac{x}{\bar{\gamma}_t}\right)^l \left[1 - \exp\left(-\frac{\bar{\gamma}_Q}{\lambda \bar{\gamma}_t}\right)\right], \quad (A.4)$$

and

$$\begin{aligned}
 I_2 &= 1 - F_{|\tilde{h}_p|^2} \left(\frac{\bar{\gamma}_Q}{\bar{\gamma}_t} \right) \\
 &\quad - \frac{\alpha}{\lambda} \exp \left(- \frac{\bar{\gamma}_Q}{\bar{\gamma}_t} \left(- \left(1 + \frac{1}{L+1} \right) \frac{(\beta - \delta)x}{\bar{\gamma}_Q} + \frac{1}{\lambda} \right) \right) \\
 &\quad \times \sum_{k=0}^{m-1} \sum_{l=0}^k \Xi(k, l) \left(\frac{x}{\bar{\gamma}_Q} \right)^l \sum_{i=0}^l \frac{l!}{i!} \left(\frac{\bar{\gamma}_Q}{\bar{\gamma}_t} \right)^i \\
 &\quad \times \left(\left(1 + \frac{1}{L+1} \right) \frac{(\beta - \delta)x}{\bar{\gamma}_Q} + \frac{1}{\lambda} \right)^{-l+i-1}. \quad (A.5)
 \end{aligned}$$

Thus, by substituting (A.4) and (A.5) into (A.1), we can obtain the closed-form expression of $\Pr(C_s > 0)$ for the considered network as shown in Theorem 1.

**APPENDIX B
PROOF OF THEOREM 3**

Specifically, substituting (24) into (26), we get

$$\begin{aligned}
 C_s &= \frac{\alpha}{\ln 2} \sum_{k=0}^{m-1} \sum_{l=0}^k \Xi(k, l) \left\{ \frac{1}{\bar{\gamma}_t^l} \left[1 - \exp \left(- \frac{\bar{\gamma}_Q}{\lambda \bar{\gamma}_t} \right) \right] \right. \\
 &\quad \times \underbrace{\int_0^\infty \frac{x^l}{1+x} \exp \left(- \left(1 + \frac{1}{L+1} \right) \frac{(\beta - \delta)x}{\bar{\gamma}_t} \right) dx}_{I_3} \\
 &\quad - \frac{1}{\lambda} \exp \left(- \frac{\bar{\gamma}_Q}{\lambda \bar{\gamma}_t} \right) \sum_{i=0}^k \frac{k!}{i!} \frac{\bar{\gamma}_Q^{i-l}}{\bar{\gamma}_t^i} \\
 &\quad \times \underbrace{\int_0^\infty \frac{x^l \left(\left(1 + \frac{1}{L+1} \right) \frac{(\beta - \delta)x}{\bar{\gamma}_Q} + \frac{1}{\lambda} \right)^{-k+i-1}}{(1+x) \exp \left(\left(1 + \frac{1}{L+1} \right) \frac{(\beta - \delta)x}{\bar{\gamma}_t} \right)} dx}_{I_4} \left. \right\}. \quad (B.1)
 \end{aligned}$$

By applying [30, eq. (2.3.6.9)], I_3 can be first obtained as

$$I_3 = \Gamma(l+1) U \left(l+1, l+1, \left(1 + \frac{1}{L+1} \right) \frac{(\beta - \delta)}{\bar{\gamma}_t} \right), \quad (B.2)$$

Then, according to [31, eq.(10)], we express the functions $(1+x)^{-1}$ and $\left(\left(1 + \frac{1}{L+1} \right) \frac{(\beta - \delta)x}{\bar{\gamma}_Q} + \frac{1}{\lambda} \right)^{-k+i-1}$ with respect to the Meijer-G function as

$$\begin{aligned}
 \left(\left(1 + \frac{1}{L+1} \right) \frac{(\beta - \delta)x}{\bar{\gamma}_Q} + \frac{1}{\lambda} \right)^{-k+i-1} &= \frac{\lambda^{k-i+1}}{\Gamma(k-i+1)} \\
 &\times G_{1,1}^{1,1} \left[\left(1 + \frac{1}{L+1} \right) \frac{\lambda(\beta - \delta)x}{\bar{\gamma}_Q} \middle| \begin{matrix} -k+i \\ 0 \end{matrix} \right], \quad (B.3)
 \end{aligned}$$

and

$$(1+x)^{-1} = G_{1,1}^{1,1} \left[x \middle| \begin{matrix} 0 \\ 0 \end{matrix} \right]. \quad (B.4)$$

Subsequently, substituting (B.3) and (B.4) into (B.1) along with [32, eq. (3.1)], we have

$$\begin{aligned}
 I_4 &= \frac{\lambda^{k-i+1}}{\Gamma(k-i+1)} \left(\left(1 + \frac{1}{L+1} \right) \frac{(\beta - \delta)}{\bar{\gamma}_t} \right)^{-(l+1)} \\
 &\quad \times G_{1,[1:1],0,[1:1]}^{1,1,1,1,1,1} \left[\begin{matrix} \frac{\lambda \bar{\gamma}_t}{\bar{\gamma}_Q} & \left| \begin{matrix} l+1 \\ -k+i; 0 \end{matrix} \right. \\ \frac{1}{\left(1 + \frac{1}{L+1} \right) \frac{(\beta - \delta)}{\bar{\gamma}_t}} & \left| \begin{matrix} - \\ 0; 0 \end{matrix} \right. \end{matrix} \right]. \quad (B.5)
 \end{aligned}$$

To this end, the desired result can be obtained by using (B.2) and (B.5) into (B.1).

**APPENDIX C
PROOF OF THEOREM 4**

We first apply [28, eq. (9.14.1)] to represent the confluent hypergeometric function ${}_pF_q(\cdot; \cdot; \cdot)$ as

$$\begin{aligned}
 {}_pF_q(m_1, \dots, m_p; n_1, \dots, n_q; x) &= \sum_{k=0}^\infty \frac{(m_1)_k \cdots (m_p)_k}{(n_1)_k \cdots (n_p)_k} \frac{x^k}{k!}. \quad (C.1)
 \end{aligned}$$

By using (C.1) into (16) along with help of [28, eq. (3.381.1), (8.354.1)], the asymptotic CDF of $|\tilde{h}_s|^2$ can be derived as

$$F_{|\tilde{h}_s|^2}^\infty(x) = \alpha \left(1 + \frac{1}{L+1} \right) x. \quad (C.2)$$

Thus, substituting (C.2) into (A.1) yields the I_1^∞ and I_2^∞ as

$$\begin{aligned}
 I_1^\infty &= \int_0^\mu F_{|\tilde{h}_s|^2}^\infty \left(\frac{x}{\bar{\gamma}_t} \right) f_{|\tilde{h}_p|^2}(y) dy \\
 &= \alpha \left(1 + \frac{1}{L+1} \right) \frac{x}{\bar{\gamma}_t} \left[1 - \exp \left(- \frac{\mu}{\lambda} \right) \right], \quad (C.3)
 \end{aligned}$$

and

$$\begin{aligned}
 I_2^\infty &= \int_\mu^\infty F_{|\tilde{h}_s|^2}^\infty \left(\frac{xy}{\mu \bar{\gamma}_t} \right) f_{|\tilde{h}_p|^2}(y) dy \\
 &= \alpha \left(1 + \frac{1}{L+1} \right) \frac{x}{\mu \bar{\gamma}_t} \exp \left(- \frac{\mu}{\lambda} \right) (\lambda + \mu). \quad (C.4)
 \end{aligned}$$

Then, substituting (C.3) and (C.4) into (A.1), we have the asymptotic CDF of γ_d as

$$\begin{aligned}
 F_{\gamma_s}^\infty(x) &= \alpha \left(1 + \frac{1}{L+1} \right) \frac{x}{\bar{\gamma}_t} \left[1 - \exp \left(- \frac{\eta}{\lambda} \right) \right] \\
 &\quad + \alpha \left(1 + \frac{1}{L+1} \right) \frac{x}{\eta \bar{\gamma}_t} \exp \left(- \frac{\eta}{\lambda} \right) (\lambda + \eta). \quad (C.5)
 \end{aligned}$$

Eventually, combining (23) and (C.5), one can obtain P_{out}^∞ as shown in Theorem 3.

REFERENCES

- [1] G. Giambene, S. Kota, and P. Pillai, "Satellite-5G integration: A network perspective," *IEEE Netw.*, vol. 32, no. 5, pp. 25–31, Sep./Oct. 2018.
- [2] K. An, M. Lin, T. Liang, J.-B. Wang, J. Wang, Y. Huang, and A. L. Swindlehurst, "Performance analysis of multi-antenna hybrid satellite-terrestrial relay networks in the presence of interference," *IEEE Trans. Commun.*, vol. 63, no. 11, pp. 4390–4404, Nov. 2015.
- [3] K. An, Y. Li Yan, and T. Liang, "On the performance of cache-enabled hybrid satellite-terrestrial relay networks," *IEEE Wireless Commun. Lett.*, to be published. doi: [10.1109/LWC.2019.2924631](https://doi.org/10.1109/LWC.2019.2924631).
- [4] W. Lu, K. An, and T. Liang, "Robust beamforming design for sum secrecy rate maximization in multibeam satellite systems," *IEEE Trans. Aerosp. Electron. Syst.*, vol. 55, no. 3, pp. 1568–1572, Jun. 2019.
- [5] A. Goldsmith, S. A. Jafar, I. Maric, and S. Srinivasa, "Breaking spectrum gridlock with cognitive radios: An information theoretic perspective," *Proc. IEEE*, vol. 97, no. 5, pp. 894–914, Apr. 2009.
- [6] A. Vanelli-Coralli, *Cooperative and Cognitive Satellite Systems*. New York, NY, USA: Academic, 2015.
- [7] S. K. Sharma, S. Chatzinotas, and B. Ottersten, "Cognitive radio techniques for satellite communication systems," in *Proc. IEEE Veh. Technol. Conf. (VTC-Fall)*, Sep. 2013, pp. 1–5.
- [8] K. An, T. Liang, G. Zheng, X. Yan, Y. Li, and S. Chatzinotas, "Performance limits of cognitive uplink FSS and terrestrial FS for Ka-band," *IEEE Trans. Aerosp. Electron. Syst.*, to be published. doi: [10.1109/TAES.2018.2886611](https://doi.org/10.1109/TAES.2018.2886611).
- [9] L. B. Cardoso da Silva, T. Benaddi, and L. Franck, "Cognitive radio overlay paradigm towards satellite communications," in *Proc. IEEE Int. Black Sea Conf. Commun. Netw. (BlackSeaCom)*, Batumi, Georgia, Jun. 2018, pp. 1–5.
- [10] K. An, M. Lin, W. Zhu, Y. Huang, and G. Zheng, "Outage performance of cognitive hybrid satellite-terrestrial networks with interference constraint," *IEEE Trans. Veh. Technol.*, vol. 65, no. 11, pp. 9397–9404, Nov. 2016.
- [11] P. K. Sharma, P. K. Upadhyay, D. B. da Costa, P. S. Bithas, and A. G. Kanatas, "Performance analysis of overlay spectrum sharing in hybrid satellite-terrestrial systems with secondary network selection," *IEEE Trans. Wireless Commun.*, vol. 16, no. 10, pp. 6586–6601, Oct. 2017.
- [12] S. Maleki, S. Chatzinotas, B. Evans, K. Liolis, J. Grotz, A. Vanelli-Coralli, and N. Chuberre, "Cognitive spectrum utilization in Ka band multibeam satellite communications," *IEEE Commun. Mag.*, vol. 53, no. 3, pp. 24–29, Mar. 2015.
- [13] C.-X. Wang, X. Hong, H.-H. Chen, and J. Thompson, "On capacity of cognitive radio networks with average interference power constraints," *IEEE Trans. Wireless Commun.*, vol. 8, no. 4, pp. 1620–1625, Apr. 2009.
- [14] K. An *et al.*, "Hybrid satellite-terrestrial relay networks with adaptive transmission," *IEEE Trans. Veh. Technol.*, to be published.
- [15] K. An, M. Lin, J. Ouyang, and W.-P. Zhu, "Secure transmission in cognitive satellite terrestrial networks," *IEEE J. Sel. Areas Commun.*, vol. 34, no. 11, pp. 3025–3037, Nov. 2016.
- [16] S. Vassaki, M. I. Poulakis, and A. D. Panagopoulos, "Optimal iSINR based power control for cognitive satellite terrestrial networks," *IEEE Trans. Emerg. Tel. Tech.*, vol. 28, no. 2, pp. 1–10, Feb. 2017.
- [17] S. Vassaki, M. I. Poulakis, A. D. Panagopoulos, and P. Constantinou, "Power allocation in cognitive satellite terrestrial networks with QoS constraints," *IEEE Commun. Lett.*, vol. 17, no. 7, pp. 1344–1347, Jul. 2013.
- [18] B. Li, Z. Fei, X. Xu, and Z. Chu, "Resource allocations for secure cognitive satellite-terrestrial networks," *IEEE Wireless Commun. Lett.*, vol. 7, no. 1, pp. 78–81, Feb. 2018.
- [19] K. Guo, K. An, B. Zhang, Y. Huang, and G. Zheng, "Outage analysis of cognitive hybrid satellite-terrestrial networks with hardware impairments and multi-primary users," *IEEE Wireless Commun. Lett.*, vol. 7, no. 5, pp. 816–819, Oct. 2015.
- [20] F. Guidolin, M. Nekovee, L. Badia, and M. Zorzi, "A study on the coexistence of fixed satellite service and cellular networks in a mmWave scenario," in *Proc. IEEE ICC*, London, U.K., Sep. 2015, pp. 1–6.
- [21] M. K. Arti, "Two-way satellite relaying with estimated channel gains," *IEEE Trans. Commun.*, vol. 64, no. 7, pp. 2808–2819, Jul. 2016.
- [22] M. K. Arti, "Channel estimation and detection in satellite communication systems," *IEEE Trans. Veh. Technol.*, vol. 65, no. 12, pp. 10173–10179, Dec. 2016.
- [23] H. A. Suraweera, P. J. Smith, and M. Shafi, "Capacity limits and performance analysis of cognitive radio with imperfect channel knowledge," *IEEE Trans. Veh. Technol.*, vol. 59, no. 4, pp. 1811–1812, May 2010.
- [24] Y. Huang, F. S. Al-Qahtani, C. Zhong, Q. Wu, J. Wang, and H. M. Alnuweiri, "Cognitive MIMO relaying networks with primary user's interference and outdated channel state information," *IEEE Trans. Commun.*, vol. 62, no. 12, pp. 4241–4254, Dec. 2014.
- [25] H. Sun, F. Zhou, R. Q. Hu, and L. Hanzo, "Robust beamforming design in a NOMA cognitive radio network relying on SWIPT," *IEEE J. Sel. Areas Commun.*, vol. 37, no. 1, pp. 142–155, Jan. 2019.
- [26] F. Zhou, Z. Chu, H. Sun, R. Q. Hu, and L. Hanzo, "Artificial noise aided secure cognitive beamforming for cooperative MISO-NOMA using SWIPT," *IEEE Trans. J. Sel. Areas. Commun.*, vol. 36, no. 4, pp. 918–931, Apr. 2018.
- [27] F. Zhou, Z. Li, J. Cheng, Q. Li, and J. Si, "Robust AN-aided beamforming and power splitting design for secure MISO cognitive radio with SWIPT," *IEEE Trans. Wireless Commun.*, vol. 16, no. 4, pp. 2450–2464, Apr. 2017.
- [28] I. S. Gradshteyn and I. M. Ryzhik, *Table of Integrals, Series, and Products*, 7th ed. New York, NY, USA: Academic, 2007.
- [29] A. Abdi, W. C. Lau, M.-S. Alouini, and M. Kaveh, "A new simple model for land mobile satellite channels: First- and second-order statistics," *IEEE Trans. Wireless Commun.*, vol. 2, no. 3, pp. 519–528, May 2003.
- [30] A. P. Prudnikov *et al.*, *Integrals and Series: Volume 1: Elementary Functions*, New York, NY, USA: Gordon & Breach, 1990.
- [31] V. S. Adamchik and O. I. Marichev, "The algorithm for calculating integrals of hypergeometric type functions and its realization in REDUCE system," in *Proc. Int. Conf. Symp. Algebr. Comput.*, Aug. 1990, pp. 212–224.
- [32] R. P. Agrawal, "Certain transformation formulae and Meijer's G function of two variables," *Indian J. Pure Appl. Math.*, vol. 1, no. 4, pp. 537–551, Mar. 1970.
- [33] K. An, T. Liang, X. Yan, and G. Zheng, "On the secrecy performance of land mobile satellite communication systems," *IEEE Access*, vol. 6, pp. 39606–39620, 2018.
- [34] K. Guo, K. An, B. Zhang, Y. Huang, D. Guo, G. Zheng, and S. Chatzinotas, "On the performance of the uplink satellite multi-terrestrial relay networks with hardware impairments and interference," *IEEE Syst. J.*, vol. 13, no. 3, pp. 2297–2308, Sep. 2019.



XIAOJUAN YAN received the M.S. degree from Guangxi University, in 2014. She received the Ph.D. degree in information and communications from the Guilin University of Electronic Technology (GUET), China. She was a visiting Ph.D. student under the supervision of Prof. C.-X. Wang with Heriot-Watt University, Edinburgh, U.K., from 2016 to 2017. She is currently an Assistant Researcher with the Guangxi Ship Digital Design and Advanced Manufacturing Research Center of Engineering Technology, Beibu Gulf University. Her current research interests include satellite-terrestrial networks, cooperative communications, and non-orthogonal multiple access.



KANG AN received the B.E. degree in electronic engineering from the Nanjing University of Aeronautics and Astronautics, Nanjing, China, in 2011, the M.E. degree in communication engineering from the PLA University of Science and Technology, Nanjing, in 2014, and the Ph.D. degree in communication engineering from Army Engineering University, Nanjing, in 2017. Since January 2018, he has been with the National University of Defense Technology, Nanjing, where he is currently an Engineer. His current research interests include satellite communication, 5G mobile communication networks, and cognitive radio.



security, cooperative communication, and cognitive networks.

TAO LIANG received the Ph.D. degree in computer science and technology from the Nanjing Institute of Communications Engineering, Nanjing, China, in 1998. He is currently a Research Fellow with the 63rd Research Institute, National University of Defense Technology, and also with the Nanjing Telecommunication Technology Institute, Nanjing. His research interests include satellite communication, digital signal processing in communications, physical layer



ZHIQIANG FENG received the Ph.D. degree in design and manufacture of ships and marine structures from Shanghai Jiao Tong University, Shanghai, China, in 2012. He is currently a Professor with the Guangxi Ship Digital Design and Advanced Manufacturing Research Center of Engineering Technology, Beibu Gulf University. His research interests include digital signal processing in communications, advanced manufacturing technology, and machine learning.

• • •



communications, edge caching, full duplex radio, wireless power transfer, cooperative communications, cognitive radio, and physical-layer security. He was a best recipient of the 2013 IEEE Signal Processing Letters Best Paper Award and the 2015 GLOBECOM Best Paper Award. He currently serves as an Associate Editor for the IEEE COMMUNICATIONS LETTERS.

GAN ZHENG (S'05–M'09) received the B.Eng. and M.Eng. degrees in electronic and information engineering from Tianjin University, China, in 2002 and 2004, respectively, and the Ph.D. degree in electrical and electronic engineering from The University of Hong Kong, Hong Kong, in 2008. He is currently a Senior Lecturer with the Wolfson School of Mechanical, Electrical and Manufacturing Engineering, Loughborough University, U.K. His research interests include UAV